Evaluation of Two Types of Dual-Frequency Differential GPS Techniques under Anomalous Ionosphere Conditions

Hiroyuki Konno, Sam Pullen, Jason Rife, and Per Enge
Stanford University

ABSTRACT

Strong ionosphere storms are a potential threat for the Local Area Augmentation System (LAAS). During these storms, large spatial and temporal gradients of the ionosphere component on the GPS signals could cause significant errors in user position estimation. Mitigating these errors is demanding for LAAS, especially for Category III LAAS.

Dual-frequency GPS techniques are known to be an effective means of reducing or removing ionosphere-induced errors and thus improving the robustness of LAAS to ionosphere anomalies. We selected two dual-frequency methods and examined their effectiveness against anomalous ionosphere situations. These two methods are divergence-free smoothing (denoted here as "DFree") and ionosphere-free smoothing (denoted here as "IFree"). These methods have the same filter structure as the single-frequency carrier-smoothing methods used in conventional single-frequency LAAS. Accordingly, we can compare the results of these methods directly to single-frequency LAAS under consistent assumptions.

In order to investigate the effectiveness of DFree and IFree, we evaluated the availability of these methods under various ionosphere conditions. Simulation results show that DFree would provide much better availability than IFree under nominal ionosphere conditions and under most anomalous conditions. However, IFree proved to be superior under extremely anomalous ionosphere conditions. Therefore, optimal availability would be obtained by implementing both DFree and IFree in real-time and switching between them based on an ionosphere monitor's best estimate of the current ionosphere state.

This paper begins by introducing the theory of DFree and IFree and then evaluates the availability of both methods under different ionosphere conditions. This evaluation is followed by a discussion of the concept of a dual-frequency LAAS architecture in which both DFree and IFree are utilized.

1.0 INTRODUCTION

Anomalous behavior of the ionosphere during strong ionosphere storms is difficult to model at the level of precision needed for the Local Area Augmentation System (LAAS). Ionosphere anomalies are thus regarded as an event that potentially threatens the integrity of LAAS. LAAS may suffer two different problems during ionosphere anomalies. One of them is caused by the large spatial gradient of the ionosphere distribution. Local-area differential GPS (DGPS) systems such as LAAS assume near-perfect correlation of ionosphere between the ground station and users. Large spatial gradients during ionosphere anomalies may make this basic assumption inappropriate. In other words, the ionosphere difference between the ground station and the user may become large enough to result in a significant position error for the user [1].

The other potential effect of the ionosphere anomalies is due to a large temporal gradient of the ionosphere component in the measurements. LAAS uses carrier smoothing to reduce the effect of multipath and thermal noise in the measurements. In the method, not only the "random noise" (multipath and thermal noise) but also the ionosphere component are fed into a low-pass filter; hence, the ionosphere divergence in the measurements induces "delay" into the smoothing process. This "delay" appears as a bias error in the smoothed measurements and, if unmitigated, could be a significant error source for user positioning [2].

It is generally thought that dual-frequency techniques will liberate DGPS systems from ionosphere-induced problems, and several methods for doing this have been introduced and evaluated as a key technology for a future CAT III

LAAS [3,4,5]. In this study, we selected two dual-frequency carrier smoothing techniques and examined them under various ionosphere conditions. The methods we selected are divergence-free smoothing (DFree) and ionosphere-free smoothing (IFree), which were well-studied in [3] and [5]. In order to maximize their ability to work with conventional single-frequency LAAS, these methods use the same filter structure as the single-frequency carrier-smoothing method used in LAAS. Hence, in the evaluation of these methods, we can employ some ideas which have been developed in research on single-frequency LAAS. For example, the methodology used to describe user position error for these methods follows the one used in single-frequency LAAS. Moreover, the receiver error models developed in research on single-frequency LAAS [6] can be used with small modifications.

The main difference of DFree and IFree is the degree to which ionosphere effects are removed from the measurements. DFree removes temporal gradients of the ionosphere delay. As mentioned above, the nuisance effect due to temporal gradients is the bias error resulting from code-carrier divergence in the smoothing process. In order to eliminate this error, DFree uses dual-frequency carrier measurements to smooth the code measurements. Using a linear combination of carrier measurements on two frequencies, this method removes the mechanism inducing the "delay" effect in the smoothing process. As a consequence, the smoothed measurements contain the same ionosphere component as the unsmoothed ("raw") code measurement without any bias errors. This method is therefore robust against ionosphere temporal gradients. However, since the raw-code ionosphere delay remains in the smoothed measurements, large ionosphere spatial gradients are still potential threats.

In contrast, IFree completely liberates us from ionosphere-induced problems. Using dual-frequency carrier and code measurements, all ionosphere components are removed from the smoothing filter. Hence, neither spatial nor temporal gradients affect the system. The primary drawback of this method is the noisy outputs from the smoothing filter. Since it uses a linear combination of dual-frequency code measurements, the filter outputs include code errors on two frequencies and are thus much noisier than the outputs of DFree, in which only single-frequency code is used.

In this paper, the effectiveness of DFree and IFree against ionosphere anomalies is examined by evaluating the availability of these methods under various ionosphere conditions. First, the availability of IFree is evaluated. As noted above, IFree is immune to ionosphere decorrelation regardless of its severity. Thus, the availability of IFree is only a function of the receiver error models and the specified vertical alert limit (VAL). The availability of IFree is evaluated for various receiver error models and VALs. These simulations indicate that IFree cannot achieve reasonable availability for CAT III with a ground receiver error model of GAD-C, an airborne receiver-error-model of AAD-B, and a VAL of 5.3 m. However, it also shows that IFree availability will increase to above 99% if the required VAL is increased to the 10-meter CAT I value and better receivers (i.e., those with one-sigma errors half that of the standard receiver error model) are used.

Next, we compare the availability of IFree and DFree under various ionosphere scenarios. In contrast with IFree, the availability of DFree varies with the ionosphere situation. For the computation of DFree availability, we assume perfect knowledge of the ionosphere condition. In other words, we set the ionosphere spatial gradient as a simulation parameter and use it as a deterministic value in the computation of DFree availability. This simulation shows that the availability of DFree is better than that of IFree for nominal gradients as well as disturbed but not extreme gradients. This is because the receiver error model for DFree is significantly smaller than that of IFree (remember that the output of the IFree smoothing filter is noisier than the output of DFree). However, as the gradient increases, DFree availability deteriorates because of the impact of the un-removed spatial gradient. For very high spatial gradients, DFree availability is overtaken by that of IFree.

The fact that both DFree and IFree are optimal under different ionosphere scenarios suggests that optimal dual-frequency system availability would be obtained by implementing both DFree and IFree in real-time and switching between them based on the ionosphere monitor's best estimate of the current ionosphere condition. In other words, we would use DFree under nominal or low-level anomalous ionosphere conditions and switch to IFree if evidence of extreme ionosphere conditions were discovered. We call this system architecture "hybrid dual-frequency LAAS". In this paper, we will discuss this concept in detail.

2.0 CARRIER-SMOOTHING ALGORITHMS

Both DFree and IFree can be characterized as carrier-smoothing methods analogous to the single-frequency carrier smoothing filter used for conventional LAAS. The main objective of carrier smoothing method is to "average out" large random errors on code measurements by using the much-less-noisy carrier measurements as aiding information. This section begins by explaining the mechanism by which carrier smoothing eliminates high-frequency noise from code measurements. After that, it derives the three filters of interest: the single-frequency carrier-smoothing filter, the DFree filter, and the IFree filter. These derivations show how the ionosphere component in code and carrier measurements behaves in the filtering

process. More detailed discussion can be found in [3].

2.1 Carrier-Smoothing Process

The task of the carrier-smoothing filter is to reduce the high-frequency noise of the measurements while avoiding tampering with the dynamic quantities of interest. For GPS navigation, the quantity of interest is the range to the satellite, which is involved in both the code measurement and the carrier measurement. The carrier-smoothing filter uses this measurement redundancy to accomplish this goal.

The basic structure of the carrier-smoothing method is a complimentary filter shown in Figure 1. The input Ψ represents the one containing code measurements, and the input Φ represents the one containing carrier measurements. As illustrated in Figure 1, the code input and the carrier input are differenced before being fed into the low-pass filter.

$$\chi = \Psi - \Phi \tag{1}$$

This differenced signal, χ, is called code-minus-carrier (CMC) and includes only "out-of-interest" components such as random noise and ionosphere. Consequently, the low-pass filter, F, operates only on the "out-of-interest" component without affecting the component of interest—the range to satellite. Conventionally, the low-pass filter is implemented as follows.

$$\bar{\chi}(t+1) = \frac{\tau - 1}{\tau}\bar{\chi}(t) + \frac{1}{\tau}\chi(t+1) \tag{2}$$

Here, τ is the smoothing time constant. The Laplace-domain expression of this low-pass filter is the following.

$$\begin{aligned} \bar{\chi}(s) &= F(s)\chi(s) \\ F(s) &= \frac{1}{\tau s + 1} \end{aligned} \tag{3}$$

The smoothed CMC, $\bar{\chi}$, is finally combined with the carrier measurement to restore the quantity of interest to the output.

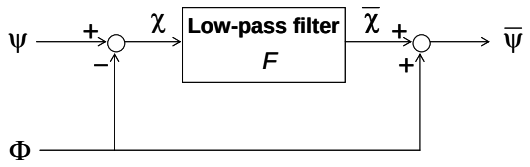

Figure 1: Complementary Filter Used in Carrier-Smoothing Method

$$\bar{\Psi} = \bar{\chi} + \Phi \tag{4}$$

The input-output relationship of the smoothing filter is obtained by combining (1), (2), and (4) after rearranging terms.

$$\bar{\Psi}(t+1) = \frac{1}{\tau}\Psi(t+1) + \frac{\tau - 1}{\tau}(\bar{\Psi}(t) + \Phi(t+1) - \Phi(t)) \tag{5}$$

Keeping this basic structure and varying the input signals, we can construct the three filters: the single-frequency carrier-smoothing filter, the DFree filter, and the IFree filter. In other words, we can implement all three of these filters by substituting different inputs Ψ and Φ into (5).

2.2 Single-Frequency Carrier Smoothing

The single-frequency carrier-smoothing filter uses the code measurement, ρ_1, for Ψ and the carrier measurement, ϕ_1, for Φ. These signals are expressed as follows.

$$\begin{aligned} \Psi &= \rho_1 = r + I_1 + \eta_1 \\ \Phi &= \phi_1 = r - I_1 + N_1 \end{aligned} \tag{6}$$

Here r includes all common terms between code and carrier, such as range to the satellite, clock offsets, and troposphere delay. I_1 represents the ionosphere component, η_1 is the random noise on code measurements (thermal noise and multipath), and N_1 is the integer ambiguity of the carrier measurements. The random noise on carrier measurements is ignored, since it is much smaller than that on code measurements. The subscript "1" indicates that the measurement is on the L1 frequency.

Substituting the signal model (6) into equation (1), the CMC variable, χ, is obtained by

$$\chi = 2I_1 + \eta_1 - N_1. \tag{7}$$

Feeding this CMC into the low-pass filter, F, and combining the smoothed CMC with the carrier measurement gives the smoothed code-measurement (the output), $\bar{\Psi}$.

$$\bar{\Psi} = r + (2F - 1)I_1 + F\eta_1 \tag{8}$$

On the right-hand side of equation (8), the first term includes the quantity of interest (the range to the satellite being tracked), the second term represents the filtered ionosphere component, and the third term represents the filtered random noise.

We can investigate the effect of the ionosphere component

by considering the second term in (8) in more detail. If the ionosphere component on the input signal is constant, the low-pass filter does nothing to it (i.e., $(2F-1)I_1 = I_1$). However, if the ionosphere has time variation, the low-pass filter induces a "delay" effect. To observe this "delay" effect, let us examine a case that the ionosphere component has a constant temporal gradient, I_d.

$$I_1(t) = I_d t + I_0 \quad . \tag{9}$$

The steady-state behavior of the filtered ionosphere component can be theoretically analyzed using the low-pass filter model in (2) or (3). Feeding the ionosphere model in (9) into the low-pass filter, we obtain the following filtered ionosphere (further details can be found in [3]).

$$\text{Filtered Ionosphere}: \; I_1 - 2\tau I_d \tag{10}$$

The second term on the right-hand side of (10) represents the "delay" effect due to the ionosphere divergence. Note the factor-of-2 multiplier, which is due to the fact that the ionosphere affects code and carrier measurements equally but in opposite directions, as shown in (6).

LAAS assumes strong correlation of the ionosphere component between the ground station and users. In other words, it assumes that the filtered ionosphere (10) for the ground station is almost identical with the one for the user. However if there exists a large spatial gradient of ionosphere between the ground station and users, the gradient might cause a hazardously large user position error. Moreover, the model (10) implies that, if the temporal variation of the ionosphere is different between the ground station and user, it will create an additional error source for user positioning.

2.3 Ionosphere Variation with Frequency

As will be seen in the next sections, DFree and IFree reduce or completely eliminate these ionosphere-induced errors. The theory behind these methods is based on the following model of ionosphere variation with signal frequency:

$$I_1 = \frac{k}{f_{L1}^2} \quad ,$$

$$I_2 = \frac{k}{f_{L2}^2} \quad ,$$

$$I_1 - I_2 = \left(1 - \frac{f_{L1}^2}{f_{L2}^2}\right) I_1 \equiv \alpha I_1 \quad , \tag{11}$$

where f_{L1} and f_{L2} are the L1 and L2 frequencies, respectively. In this paper, we use the L2 signal as the second signal; however, the discussions below are completely applicable to the use of other frequencies such as L5.

2.4 Divergence-Free Smoothing (DFree)

DFree corrects for the effects of temporal gradients of the ionosphere component. As mentioned above, the nuisance effect of temporal gradients is basically caused by the ionosphere component being fed into a low-pass filter. The idea of DFree is to cancel out the ionosphere component before the signals pass through the low-pass filter. To accomplish this, DFree uses the following signals as inputs to the filter in Figure 1. The DFree filter is then implemented by substituting these signals into equation (5).

$$\begin{aligned} \Psi &= \rho_1 \\ \Phi &= \phi_1 - \frac{2}{\alpha}(\phi_1 - \phi_2) \end{aligned} \tag{12}$$

Using the measurement signal model in (6) and the ionosphere model in (11), the carrier input in (12) is expressed as:

$$\Phi = r + I_1 + N_1 - \frac{2}{\alpha}(N_1 - N_2) \, . \tag{13}$$

As can be seen in this equation, the linear combination of dual-frequency carrier measurements extracts the positive ionosphere component in the carrier input. Accordingly, the difference of the code input and the carrier input generates "ionosphere-free" CMC.

$$\chi = \Psi - \Phi = \eta_1 - N_1 + \frac{2}{\alpha}(N_1 - N_2) \tag{14}$$

Feeding this CMC into the low-pass filter, F, and then adding the carrier input to the smoothed CMC, we finally obtain the smoothed code measurements expressed as:

$$\overline{\Psi} = r + I_1 + F\eta_1 \, . \tag{15}$$

Note that the "delay" effect due to ionosphere divergence has vanished from the output.

Because of this robustness against ionosphere divergence, DFree is a powerful technique for next generation DGPS, and some research has been done on it [3,5]. However, since the raw-code ionosphere component, I_1, remains in the smoothed measurements, large spatial gradients are still potential threats for this method.

2.5 Ionosphere-Free Smoothing (IFree)

IFree is a smoothing method that completely removes all ionosphere-induced errors. IFree employs the following linear combinations of dual-frequency code measurements and dual-frequency carrier measurements. Implementation of the IFree filter is done by substituting these signals into

equation (5).

$$\Psi = \rho_1 - \frac{1}{\alpha}(\rho_1 - \rho_2)$$
$$\Phi = \phi_1 - \frac{1}{\alpha}(\phi_1 - \phi_2) \quad (16)$$

These linear combinations generate "ionosphere-free" signals using the signal model in (6) and the ionosphere model in (11).

$$\Psi = r + \eta_1 - \frac{1}{\alpha}(\eta_1 - \eta_2)$$
$$\Phi = r + N_1 - \frac{1}{\alpha}(N_1 - N_2) \quad (17)$$

Passing these inputs through the filter in Figure 1, we obtain the smoothed measurements expressed as:

$$\overline{\Psi} = r + F(\eta_1 - \frac{1}{\alpha}(\eta_1 - \eta_2)). \quad (18)$$

This output contains no ionosphere-related terms at all.

Since IFree is perfectly immune to ionosphere-related problems, it appears on the surface to be a better method than DFree. However, the drawback of IFree is the large noise on the smoothed measurements. Since IFree uses dual-frequency code measurements in (16) as inputs, the outputs are influenced by code errors on two frequencies and are therefore much noisier than the outputs of DFree, in which only single-frequency code measurements are used. The relative superiority of DFree and IFree depends on whether, for a given ionosphere state, the increased measurement noise from IFree has a greater impact on LAAS system performance than the retention of ionosphere code impacts in DFree. In the next section, we will provide an answer to this question from the viewpoint of LAAS system availability.

3.0 AVAILABILITY ASSESSMENT OF DFree AND IFree

In order to calculate the availability of DFree and IFree, we need to construct error models for each method. Hence, this section starts with the derivation of these error models. After that, it explains how availability is calculated. Finally, the results of availability simulations under various ionosphere conditions are introduced.

3.1 System Error Model

The availability of LAAS is judged by comparing the position-estimation error bound (at a rare-event probability derived from the LAAS integrity requirements) with a required error limit based on the "safe zone" that applies to a given LAAS operation. This error bound is called a Protection Level (PL), and the limit it is compared to is called an Alert Limit (AL). Since the vertical direction is the constraining direction for approach and landing operations, in this paper, we consider only the Vertical Protection Level (VPL) and the Vertical Alert Limit (VAL).

In the RTCA Minimum Aviation System Performance Standards (MASPS) for LAAS [7], four VPLs are defined for different fault hypotheses. This paper focuses on the one for the fault-free, or H0, hypothesis, because this VPL (VPL_{H0}) generally dominates the other VPLs. VPL_{H0} is defined as the total error bound assuming independent Gaussian errors for each available satellite and is calculated as follows.

$$VPL_{H0} = K_{ffmd}\sqrt{\sum_{i=1}^{N} S_{v,i}^2 \sigma_i^2} \quad (19)$$

Here, the subscript i indicates a usable satellite, σ_i is the range domain error for satellite i, and the terms $S_{v,i}$ are the relevant coefficients from the weighted pseudoinverse range-to-position transformation matrix **S**. With the scaling factor K_{ffmd}, the probability that the vertical position error exceeds VPL without an alert being given to the user within a specified time-to-alert is guaranteed to be less than the required integrity risk probability [7].

The standard deviation of measurement errors for each satellite, σ_i, is the square root of the summation of error variances associated with the ground receiver, airborne receiver, and ionosphere decorrelation (troposphere decorrelation and other error sources also exist in LAAS, but these have been neglected because they are small by comparison). Specifying the sigmas for these error terms for DFree and IFree allows us to calculate VPL_{H0} for these methods.

3.1.1 Measurement-error models for DFree

For carrier-smoothing methods, the noise level of the smoothed output signals is generally governed by the code input (Ψ in Figure 1), since high-frequency noise on code measurements is much larger than that on carrier measurements. Both DFree and conventional single-frequency carrier-smoothing use L1 code measurements for their code inputs. Therefore, residual noise on the output of DFree is regarded as being of the same magnitude as the noise on the output of single-frequency carrier smoothing. Therefore the standard LAAS receiver error model [6] can be used for the DFree receiver model. Specifically, in this paper, the GAD-C4 model (here "C4" indicates that a 4-receiver configuration is assumed) is assigned to the ground receiver error, σ_{Df_gnd}, and the AAD-B model is assigned to the airborne receiver error, σ_{Df_air}.

$$\sigma_{Df\_gnd} = GAD\text{–}C4$$
$$\sigma_{Df\_air} = AAD\text{–}B \quad (20)$$

For DFree, the sigma value of ionosphere decorrelation, σ_{Df_iono}, is given as follows.

$$\sigma_{Df\_iono} = d_{gu} \cdot \sigma_{vig} \cdot Oq(el) \quad (21)$$

Here, d_{gu} is the distance between the ground station and the user, σ_{vig} is the nominal ionosphere spatial gradient in the vertical (zenith) domain, and *Oq(el)* is the obliquity factor corresponding to the elevation angle *el*.

The total measurement error of DFree, σ_{Df}, is given by the root-sum-square of these terms.

$$\sigma_{Df} = \sqrt{\sigma^2_{Df\_gnd} + \sigma^2_{Df\_air} + \sigma^2_{Df\_iono}}$$

Substituting this model into equation (19), VPL_{H0} for DFree is computed as follows.

$$VPL_{H0\_Dfree} = K_{ffmd}\sqrt{\sum_{i=1}^{N} S^2_{v,i}(\sigma^2_{Df\_gnd,i} + \sigma^2_{Df\_air,i} + \sigma^2_{Df\_iono,i})} \quad (22)$$

3.1.2 Measurement error models for IFree

In contrast to DFree and single-frequency carrier smoothing, IFree employs a linear combination of L1 and L2 code measurements as its code input (see equation (16)). Assuming that the errors on L1 and L2 code measurements are independent, the residual error on the smoothed signal, $\sigma_{If\_residual}$, is expressed as:

$$\sigma_{If\_residual} = \sqrt{\left(1-\frac{1}{\alpha}\right)^2\sigma_1^2 + \frac{1}{\alpha^2}\sigma_2^2}\ , \quad (23)$$

where σ_1 denotes the sigma of residual error for smoothed L1 code, and σ_2 denotes that for smoothed L2 code (recall that the definition of α is given in (11)). For simplicity, we assume that σ_1 and σ_2 are identical. Accordingly, the receiver error models for IFree—σ_{If_gnd} for the ground receiver and σ_{If_air} for the airborne receiver—are given by:

$$\sigma_{If\_gnd} = \sqrt{1-\frac{2}{\alpha}+\frac{2}{\alpha^2}}\ GAD\text{–}C4$$
$$\sigma_{If\_air} = \sqrt{1-\frac{2}{\alpha}+\frac{2}{\alpha^2}}\ AAD\text{–}B \quad . \quad (24)$$

For the L1/L2 combination, the inflation factor applied to the standard models is about 2.98.

Since IFree is not affected by ionosphere, the total measurement error of IFree contains only ground and airborne receiver errors. Using these errors, VPL_{H0} for IFree is computed as follows.

$$VPL_{H0\_Ifree} = K_{ffmd}\sqrt{\sum_{i=1}^{N} S^2_{v,i}(\sigma^2_{If\_gnd,i} + \sigma^2_{If\_air,i})} \quad (25)$$

3.2 Availability Computation

System availability is computed as the average of "instantaneous" availability for all possible satellite geometries during a 24-hour day of repeatable GPS geometries [8,9]. In this paper, the standard 24-satellite constellation defined in [10] is used to obtain the satellite position. The system availability, P_{avail}, is computed by the following equation.

$$P_{avail} = \sum_{l=1}^{L}\frac{1}{L}\left[\sum_{Q=0}^{3}\sum_{m=1}^{M(Q)}\frac{P_{SVout}(Q)}{M(Q)}P_{avail-idc}(\lambda_m(t_l,Q))\right] \quad (26)$$

Here, $P_{avail\text{-}idc}(\lambda_m(t_l,Q))$ is the availability indicator for a satellite geometry $\lambda_m(t_l,Q)$. It takes 1 if the system is available for the geometry, otherwise it takes 0. The way to decide the value of $P_{avail\text{-}idc}(\bullet)$ will be described later. The inside of the brackets in equation (26) corresponds to the instantaneous availability at a particular epoch t_l (l = 1,…, L). This instantaneous availability is a weighted-average of the availability indicators for all possible satellite geometries at the epoch, which geometries include those for which one or more satellites are unavailable. The parameter Q represents the number of unavailable satellites, and $M(Q)$ is the number of satellite-combinations that occur for the Q-satellite-out condition (i.e., $M(Q)$ = "24 choose Q"). For each of these combinations, a geometry of visible satellites, $\lambda_m(t_l,Q)$, is defined, and the availability indicator for this geometry, $P_{avail\text{-}idc}(\lambda_m(t_l,Q))$, is specified—$M(Q)$ availability indicators are totally computed for the Q-satellite-out case. The instantaneous availability is computed by averaging these availability indicators with a weighting-factor $P_{SVout}(Q)/M(Q)$. Here, $P_{SVout}(Q)$ is the probability that Q satellites are unavailable, and we use a "historical" probability [8] listed in Table 1. Finally, the instantaneous availabilities are uniformly averaged for all epochs (t_l: l = 1,…, L).

The availability indicator $P_{avail\text{-}idc}(\lambda_m)$ is specified based on two criteria.

$$P_{avail-idc}(\lambda_m) = \begin{cases} 1 & \text{two criteria met} \\ 0 & \text{otherwise} \end{cases} \quad (27)$$

Table 1: Historical Probability Weights

Unavailable Satellites, Q, in 24 Satellite Constellation	Probability Weight $P_{SVout}(Q)$
0	9.85056×10^{-1}
1	1.4839×10^{-2}
2	1.04×10^{-4}
3	1.0×10^{-6}
4+	0

The first criterion is that, for the given geometry, VPL must be lower than the required VAL (e.g., CAT I LAAS currently requires a 10-meter VAL [7]). This criterion is assessed simply by comparing the instantaneous VPL computed by equation (19) to VAL.

The second criterion is that the given geometry must have no more than a certain number of critical satellites in order to meet the continuity requirements (e.g., CAT I LAAS requires an upper limit of 6 critical satellites [7]). A critical satellite is one whose failure will cause the updated VPL to exceed VAL (assuming that nothing else changes), which would cause an operation in progress to be aborted. For each satellite geometry, λ_m, the presence of critical satellites can be determined by sequentially removing a satellite, one at a time, and comparing VPL to VAL for each reduced satellite set. A satellite whose removal leads VPL larger than VAL is a critical satellite, and if the number of such satellites in a particular satellite geometry is more than the limit, that geometry is regarded unavailable (i.e., $P_{avail\text{-}idc}(\lambda_m) = 0$).

3.3 Availability evaluation for IFree

As mentioned above, instantaneous availability depends on VPL_{H0} and VAL, and VPL_{H0} for IFree depends only on the ground and airborne receiver models. The availability of IFree is thus considered as a function of the receiver models and VAL. In order to study the performance of IFree, we evaluated its availability with various receiver models and various VALs.

The IFree receiver models are given by (24). We constructed simulation models for both the ground receiver and the airborne receiver by inflating the standard receiver models, GAD-C4 and AAD-B, with a range of scale factors. Three scale factors for the ground receiver (0.5, 0.75, and 1.0) and four scale factors for the airborne receiver (0.25, 0.5, 0.75, and 1.0) were chosen—these models are plotted in Figures 2 and 3. For reference, the original GAD-C4 and AAD-B curves are also plotted in these figures with dashed lines. The large error present in IFree outputs can be confirmed in these plots. For VAL, we selected 3 values: 10 m, 7.5 m, and 5.3 m. Here, the 10 meter VAL corresponds to the current CAT I requirement in [7], and the 5.3-meter VAL corresponds to the CAT III requirement in the previous (September 1998) version of [7].

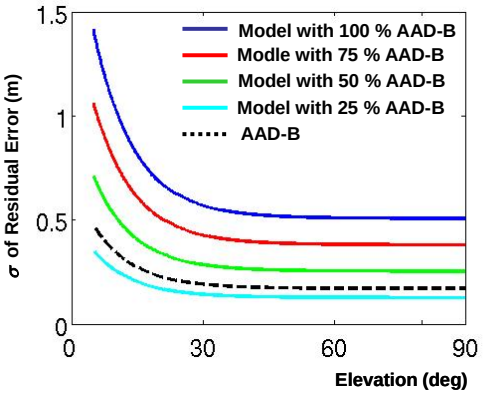

Figure 2: Airborne Receiver Models for IFree

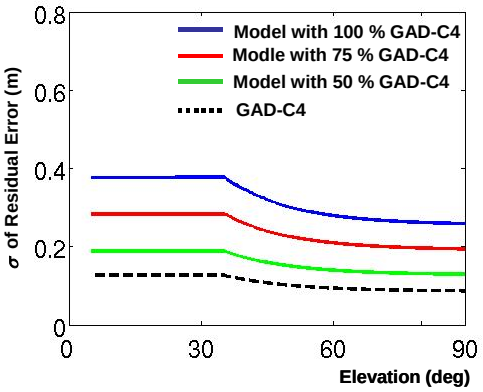

Figure 3: Ground Receiver Models for IFree

Combining these receiver models and VALs creates a total of 36 ($3 \times 4 \times 3$) simulation conditions. For each condition, the availabilities for 20 airports in the conterminous United States (CONUS) were computed using 5-minute sampling intervals and the standard 24-satellite constellation defined in [10] (the sample number, L in equation (26), thus equals 288). Other system parameters necessary to the availability computation were set based on the CAT III requirement and are listed in Table 2.

Table 2: Other Simulation Parameters

Fault-free missed detection multiplier K_{ffmd}	6.673
Maximum number of critical satellites	2

From these 36 conditions, the simulations for the standard receiver models (i.e., GAD-C4 and AAD-B with scaling factors of 1.0) and the conditions with an availability greater than 95 % are shown in Table 3. Each availability result corresponds to the worst availability found over the 20 airports. As can be seen in Table 3, the standard receiver models provide unacceptably low availability. Even with the CAT I VAL of 10 m, these models achieve only 68.5 % availability. Therefore, improved receiver error models are indispensable for IFree.

Regarding these error models, the dominance of airborne receiver error in the availability computation is another interesting point. Comparing the airborne receiver model and the ground receiver model (Figures 2 and 3, respectively), it is clear that the airborne model has larger error than the ground model (especially for low-elevation satellites). In the simulations, the effect of the larger error appears as the sensitivity of availability improvement as airborne receiver error is lowered. As shown in Table 3, for the same 10-meter VAL, the combination of 75% GAD-C4 and 50% AAD-B provides higher availability than the combination of 50% GAD-C4 and 75% AAD-B. Therefore, improved airborne receivers (and/or lower airborne multipath) are key to improving the availability of IFree.

The simulations also show that some relaxation of VAL is essential. For a 5.3-meter VAL, the maximum availability achieved by the best receiver combination (50% GAD-C4 and 25% AAD-B) is 98.4%. On the other hand, for a 10-meter VAL, availability above 99% is achieved by 50% error levels for both receivers. To obtain 99% availability with a 7.5-meter VAL, the error level of the airborne receiver has to be reduced to 25% of the current model. These results imply that relaxing the CAT III VAL to 10 m, as suggested in the updated RTCA LAAS MASPS [7], is needed for IFree.

Table 3: Availability of IFree under Various Simulation Conditions

Ground Receiver	Airborne Receiver	VAL (m)	Availability (%)
100% GAD	100% AAD	5.3	0.001
100% GAD	100% AAD	7.5	8.539
100% GAD	100% AAD	10	68.513
100% GAD	50% AAD	10	97.674
100% GAD	25% AAD	10	99.477
75% GAD	50% AAD	10	99.510
75% GAD	25% AAD	7.5	99.135
75% GAD	25% AAD	10	99.925
50% GAD	75% AAD	10	96.246
50% GAD	50% AAD	7.5	98.018
50% GAD	50% AAD	10	99.901
50% GAD	25% AAD	5.3	98.440
50% GAD	25% AAD	7.5	99.935
50% GAD	25% AAD	10	99.977

If the 10-meter VAL is approved for CAT III, IFree would provide more than 99.9% availability with ground and airborne receivers whose one-sigma errors are 50% of the current receiver error models. Here, a question arises. Are 50% error reductions in both ground and air feasible?

For ground receivers, one means for noise reduction is to increase the time constant of the smoothing filter (τ in equation (5)). Theoretically, inflating the time constant by a factor of 4 attenuates the noise by half [3]. GAD-C4 is based on τ of 200 samples (which is equivalent to a 100-second time constant because of the 2-Hz measurement update rate of LAAS). Hence, 50% GAD-C4 might be accomplished with an 800-sample, or 400-second, time constant. Because of the capability of removing ionosphere divergence or ionosphere itself from the output signal, DFree and IFree enable receivers to use very long time constant to significantly reduce the random noise. On the other hand, it is inappropriate for single-frequency carrier-smoothing filter to use a long time constant, since the ionosphere divergence proportionally increases with the time constant [2,3].

Because of the recovery time needed after a loss-of-lock, such a long time constant may be unacceptable for airborne receivers. However, it may not be necessary. Murphy, *et al*. conducted a series of flight tests to obtain actual multipath data for several Boeing airplane models with a 100-second smoothing filter (see [11]). Analysis of this data showed that the AAD-B error model had a large margin for the low-elevation region (0 - 25 deg) and the high-elevation region (60 - 90 deg). In particular, the empirical data was almost half of AAD-B at the low elevation region. Since AAD-B has relatively high errors in the low-elevation region, if this segment of the model could be tightened based on the empirical data, it would significantly improve IFree availability with the current standard 100-second smoothing time constant.

Employing L5 (1176.45 MHz) as the second signal will also contribute to error reduction. For the L1/L5 combination, the inflation factor applied to the standard model in the IFree model (square-root term in equations (23)) falls to 2.59, compared to 2.98 for the L1/L2 combination. Moreover, L5 receivers are likely to have smaller residual errors on smoothed code measurements than L1 receivers because of the wider bandwidth of the L5 signal compared to L1. Wider bandwidth enables L5 receivers to use a narrower correlator for code measurements than that of L1 receivers. Consequently, L5 receivers will suffer less from multipath effect than L1 receivers. This error reduction would appear as σ_2 less than σ_1 in the IFree error model (equation (23)), whereas this paper assumes these values to be same. The effectiveness of narrow correlators was also confirmed in [11].

Based upon the above discussions, we conclude that high-quality receivers such as those with one-sigma errors half that of current standard receivers will likely be feasible in the near future. Thus IFree could be a practical method when combined with such high-quality receivers and a 10-meter VAL.

3.4 Comparison of IFree and DFree

Under nominal ionosphere conditions, the total system error of DFree is much smaller than that of IFree, since, as noted before, the receiver error of DFree is much smaller than that of IFree (compare equations (20) and equations (24)). On the other hand, if a large ionosphere gradient exists between the ground station and the user, and if the gradient is known to exist and is modeled in availability determination, the availability of DFree will deteriorate due to the un-removed absolute ionosphere error between ground and airborne receivers. Thus, at a sufficiently large ionosphere gradient, this "true" DFree availability would fall below the IFree availability, which remains the same regardless of the ionosphere condition. This section investigates what level of anomalous ionosphere gradient is required for IFree to become superior.

For DFree, an ionosphere monitor is essential to maintain system integrity. The ionosphere term in the DFree error model (σ_{Df_iono} in equation (22)) bounds ionosphere errors only under nominal conditions. Large ionosphere gradients could thus cause integrity failure unless a monitor notifies the user that the standard VPL equations do not apply to the current situation. In order to maintain integrity, the monitor should be conservative; however, if it is over-conservative, the system loses availability more than is necessary. Therefore, the availability of DFree depends highly on the *sensitivity* and *selectivity* of the ionosphere monitor.

As the first step in studying DFree availability under anomalous ionosphere conditions, DFree availability was evaluated assuming a "perfect" ionosphere monitor. In other words, we assumed perfect knowledge of the ionosphere gradient in the availability computation so that the theoretically maximum availability could be achieved for each ionosphere condition. This approach maximizes the utility of DFree relative to IFree. In practice, because protecting integrity far outweighs maximizing availability, IFree will be preferred over DFree under a wider range of conditions than this analysis suggests.

To implement this "perfect" monitor, the VPL_{H0} equation for DFree (equation (22)) is modified to:

$$VPL_{H0\_Dfree} = K_{ffmd}\sqrt{\sum_{i=1}^{N} S_{v,i}^2(\sigma_{Df\_gnd,i}^2+\sigma_{Df\_air,i}^2)}+\left|\sum_{j=1}^{M} S_{v,j}\frac{\partial I_j}{\partial x}d_{gu}\right|, \quad (28)$$

where $\partial I_j / \partial x$ is the actual spatial gradient of ionosphere in the slant domain with respect to satellite j, and d_{gu} is the distance between the ground station and the user. The last term of this equation shows the perfect knowledge of the ionosphere errors which would be obtained by the "perfect" monitor. More specifically, the monitor says that, for satellite j (j = 1,…, M), there is an ionosphere spatial gradient whose value is $\partial I_j / \partial x$.

Figure 4 illustrates the assumed configuration of the LAAS-supported landing operation. Availability is computed at the "decision point," which is assumed to be 5 km from the ground receiver (i.e., d_{gu} = 5 km in equation (28)). For each simulation, we varied the ionosphere gradient ($\partial I / \partial x$ in equation (28)) and the number of satellites hit by the gradient (M in equation (28)). For example, Figure 4 shows the case where one satellite (Satellite A) is affected by the ionosphere gradient of α mm/km. The satellites affected by a gradient are chosen based on their sensitivity to the ionosphere error—given M affected satellites, the M satellites most sensitive to the presence of an ionosphere gradient are selected. For the case where multiple satellites are hit, this selection may not simulate an actual situation, since a single ionosphere anomaly event would most likely affect satellites based not on their sensitivity to the resulting ionosphere error but on their geometry (i.e., the gradient most likely affects satellites whose ionosphere pierce points are geometrically adjacent). Thus, this selection method is quite conservative from an integrity standpoint.

Simulations were conducted for five cases. The receiver models and VALs used for each case are listed in Table 4. Case 1 corresponds to the default CAT III condition: GAD-C4, AAD-B, and a 5.3-meter VAL. Case 2 uses the same receiver models and a relaxed VAL of 10 meters.

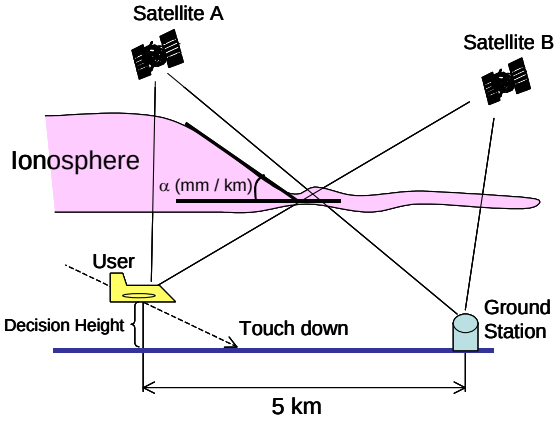

Figure 4: Illustration of Landing Operation with Ionosphere Gradient Present

Table 4: Simulation Cases

Case	Ground Receiver	Airborne Receiver	VAL (m)
1	100 % GAD-C4	100 % AAD-B	5.3
2	100 % GAD-C4	100 % AAD-B	10
3	75 % GAD-C4	50 % AAD-B	10
4	50 % GAD-C4	50 % AAD-B	10
5	50 % GAD-C4	25 % AAD-B	10

Cases 3 to 5 use the better receiver models and the 10-meter VAL under which IFree achieves reasonably high availability (see Table 3). Other system parameters necessary to the availability computation were set based on the CAT III requirement in the same manner as for the evaluation of IFree availability (see Table 2).

Tables 5 through 9 show the simulation results for each of these cases. Each row corresponds to a specific ionosphere gradient magnitude, and each column corresponds to a number of satellites affected by the gradient. The ionosphere gradient was varied from 100 mm/km to 350 mm/km (based on the ionosphere anomaly threat models discussed in [1,13]) with a 50-mm/km interval. For each gradient, the number of satellites affected by the gradient was varied from 1 to 5. Underneath the anomalous-condition results, the availability under nominal condition is also shown in each table. To compute the availability for the nominal condition, VPL_{H0} given by equation (20), (21), and (22) was used. The sigma of the nominal ionosphere spatial gradient, σ_{vig} in equation (21), was set to be 5 mm/km. The bottom row of each table shows the availability of IFree for the same scenario (recall that IFree availability is the same for each case regardless of the ionosphere condition). The yellow cells indicate the ionosphere conditions for which, under these assumptions, IFree availability is higher than DFree availability.

Table 5 shows the availability of DFree constructed with the parameters for the default CAT III LAAS requirement from the original LAAS MASPS (with the 5.3-meter VAL). As shown in the table, in this case, DFree availability is less than 99% even for nominal ionosphere conditions. On the other hand, if VAL is relaxed to 10 m, DFree achieves more than 99.9% availability for nominal conditions, as shown in Table 6. Therefore relaxation of VAL (as implied by the updated LAAS MASPS [7]) is very desirable for DFree. For these two cases, IFree is not comparable to DFree, since it attains extremely low availability.

Tables 7, 8, and 9 correspond to the cases of improved receiver error models. As with IFree, the availability of DFree increases for these better receiver models. Availability under nominal conditions is more than 99.99% for all of these cases and is much higher than that of IFree.

These results thus verify the theoretical prediction that the availability of DFree would be higher than that of IFree under nominal ionosphere conditions. Furthermore, these simulations show that DFree attains quite high availability even under anomalous conditions. For Case 3 (see Table 7), DFree provides higher availability than IFree for most of

Table 5: DFree Availability for 100% GAD, 100% AAD, and 5.3 m VAL

Iono. Grad. (mm/km)	Number of affected satellites				
	1	2	3	4	5
100	97.714	96.554	93.734	89.002	78.133
150	97.691	95.108	90.125	80.235	61.172
200	97.335	94.016	84.813	69.048	45.248
250	97.318	91.922	80.229	53.542	31.802
300	96.954	89.435	73.602	45.588	21.514
350	96.234	85.890	64.202	35.907	14.336
Availability under nominal conditions				98.707	
IFree availability				0.001	

unit of availability (%)

Table 6: DFree Availability for 100% GAD, 100% AAD, and 10 m VAL

Iono. Grad. (mm/km)	Number of affected satellites				
	1	2	3	4	5
100	99.976	99.966	99.939	99.892	99.878
150	99.974	99.958	99.904	99.504	98.105
200	99.971	99.940	99.548	99.057	95.860
250	99.967	99.919	99.170	97.302	91.859
300	99.963	99.905	99.129	96.451	88.187
350	99.962	99.883	98.712	94.289	82.889
Availability under nominal conditions				99.978	
IFree availability				68.513	

unit of availability (%)

Table 7: DFree Availability for 75% GAD, 50% AAD, and 10 m VAL

Iono. Grad. (mm/km)	Number of affected satellites				
	1	2	3	4	5
100	99.991	99.989	99.983	99.966	99.966
150	99.991	99.985	99.970	99.918	99.908
200	99.989	99.983	99.947	99.547	99.138
250	99.989	99.976	99.921	99.134	96.630
300	99.987	99.970	99.561	99.046	94.049
350	99.986	99.961	99.536	97.937	89.062
Availability under nominal conditions				99.992	
IFree availability				99.510	

unit of availability (%)

Table 8: DFree Availability for 50% GAD, 50% AAD, and 10 m VAL

Iono. Grad. (mm/km)	Number of affected satellites				
	1	2	3	4	5
100	99.992	99.991	99.984	99.971	99.970
150	99.992	99.988	99.977	99.927	99.922
200	99.991	99.985	99.963	99.555	99.518
250	99.990	99.981	99.931	99.151	97.039
300	99.989	99.974	99.899	99.066	94.770
350	99.989	99.965	99.550	98.307	90.079
Availability under nominal conditions				99.993	
IFree availability				99.901	

unit of availability (%)

Table 9: DFree Availability for 50% GAD, 25% AAD, and 10 m VAL

Iono. Grad. (mm/km)	Number of affected satellites				
	1	2	3	4	5
100	99.994	99.993	99.990	99.981	99.981
150	99.994	99.992	99.984	99.961	99.954
200	99.993	99.989	99.973	99.906	99.891
250	99.993	99.986	99.952	99.538	98.423
300	99.992	99.984	99.929	99.125	96.583
350	99.991	99.977	99.897	98.700	93.299
Availability under nominal conditions				99.997	
IFree availability				99.977	

unit of availability (%)

the anomalous ionosphere conditions examined. Only under extremely severe conditions such as a gradient of 250 mm/km affecting 4 satellites, does IFree have an advantage over DFree. The range of anomaly conditions over which IFree is superior to DFree expands as the receiver models are improved (compare Tables 7, 8, and 9). However, for the cases in which only one satellite is affected (the first column in the tables), DFree provides higher availability for all gradients. According to recent research on ionosphere storms in CONUS (see [12,13,14]), it is less likely that a large gradient will affect multiple satellites. These simulations thus suggest that DFree with a "perfect" ionosphere monitor will almost always be more effective than IFree.

Given these results, it makes sense to reconsider the assumption of a "perfect" ionosphere monitor. In practice, ionosphere monitors have uncertainty in their estimate of the current ionosphere condition; hence, they must have a conservative error margin for this estimate which margin can be shown to "overbound" this uncertainty. This error margin will likely cause a practical monitor to declare unsafe some ionosphere conditions in which the user position error is actually less than VAL. Consequently, DFree will not achieve the availability shown here in practice.

In order to investigate what amount of availability is lost due to the conservatism of the monitor, additional simulations with a specific practical monitor are required. However, the simulations in this paper show that, for the cases with the improved receiver models, the predominance of cases where DFree availability is better will be reversed with a small amount of availability loss. For Case 5 (see Table 9), which uses the lowest-error receiver pair, if DFree loses availability by only 0.02%, IFree availability will exceed DFree availability for all anomalous ionosphere conditions. For Case 4 (see Table 8), the availability advantage of DFree is less than 0.1%, and, for Case 3 (see Table 7), DFree is overtaken by IFree after a DFree availability loss of 0.5%.

Luo *et al.* analyzed the availability loss for single-frequency LAAS under anomalous ionosphere conditions using a method called "geometry screening" [1]. Several screening methods were investigated, and some "practical" ones were demonstrated to reduce availability by more than 0.5%. Since their simulations were based on the error models of single-frequency LAAS, the results cannot be easily compared with the availability loss of DFree based on our simulation scenarios. However, the results in [1] suggest that, under anomalous ionosphere conditions, DFree could lose a relatively large amount of availability by using an "imperfect" or "practical" ionosphere monitor, and the chart of the supremacy of DFree and IFree under perfect knowledge in Tables 7, 8, and 9 could drastically change.

4.0 HYBRID DUAL-FREQUENCY LAAS CONCEPT

The simulation results described in the previous section provide important information regarding the utility of the dual-frequency LAAS using DFree or IFree. These results show that, if lower-error receivers such as those with one-sigma errors half that of the current standard error models are available, and if VAL is relaxed to 10 m, DFree and IFree can operate in a complementary manner based on the ionosphere condition. With perfect information, DFree is preferable under both nominal and anomalous but not extremely anomalous ionosphere condition. On the other hand, IFree is more effective than DFree under extremely anomalous ionosphere conditions. This result suggests that optimal availability would be obtained by implementing both DFree and IFree and selecting the more-effective method in real time based on the ionosphere condition estimated by the ionosphere monitor. We call this system architecture "hybrid dual-frequency LAAS".

The concept of hybrid dual-frequency LAAS is based on the assumption of lower receiver errors and a VAL of at least 7.5 meters (preferably 10 meters). As discussed in

Section 3.3 and in [7,11], these assumptions may be realized in the next few years. If this happens, hybrid dual-frequency LAAS may be the best option for achieving a robust, high-availability "end-state" CAT III LAAS when L2C and/or L5 become available. The only thing that is required for the hybrid system that is not needed for a DFree-only system is that both ground and airborne systems must execute DFree and IFree processing simultaneously and in parallel so that both can shift from one to the other (at the same epoch in time) without interrupting navigation. While a system that uses only IFree would be simpler than either a hybrid system or a DFree-only system, the price in terms of reduced availability is prohibitive, as shown in Section 3.4.

For now, hybrid dual-frequency LAAS is a preliminary concept only. To make it a reality, the following two questions need to be answered.

(1) Can a practical ionosphere monitor be developed that is not too conservative?

(2) What is the optimal ionosphere condition threshold at which the system switches from DFree to IFree?

The simulations introduced in Section 3.4 provide preliminary answers for these questions. More specifically, the simulations show the optimal "switching-point" between DFree and IFree for a theoretical hybrid system using a "perfect" ionosphere monitor. For example, a hybrid system with 50% GAD-C4, 50% AAD-B, and a 10-meter VAL should use DFree under ionosphere conditions corresponding to the uncolored cells in Table 8. It should switch to IFree under ionosphere conditions corresponding to the yellow cells in the table.

Since the theoretical system assumes a "perfect" ionosphere monitor, the ionosphere conditions for IFree are unreasonably severe. Depending on the final ionosphere anomaly "threat model" for CAT III (i.e., a model that separates unusual but credible ionosphere conditions from conditions so extreme as to be essentially impossible), there may be no occasion that the system uses IFree if a "perfect" monitor is available. In practice, however, we cannot have a perfect ionosphere monitor. As discussed in Section 3.4, the ionosphere conditions under which IFree is preferred will expand with a "practical" ionosphere monitor. Our ongoing work thus involves designing and optimizing an implementable ionosphere monitor and assessing the availability of DFree in practice in the same manner as the assessments performed in this paper. By doing this, we will be able to examine the effectiveness of hybrid dual-frequency LAAS under real-world conditions.

5.0 CONCLUSION

This paper evaluated the DFree and IFree dual-frequency carrier-smoothing for CAT III LAAS with various receiver error models, VALs, and ionosphere conditions. Under nominal ionosphere conditions, the best performance is provided by DFree. Nevertheless, DFree with current error receiver models and the original 5.3-meter VAL achieved an availability of less than 99%, which is not sufficient for a dual-frequency "end-state" CAT III LAAS. This result strongly supports proposals to relax VAL [7,15] and the efforts to reduce the conservatism of the current receiver error models [11].

To be practical, IFree needs improved receiver error models and a relaxed VAL even more than DFree does. The simulation results in this paper show that IFree would be essentially worthless with the current receiver error models and a 5.3-meter VAL. However, these results also showed that IFree could achieve reasonably high availability with better receiver error models and a relaxed VAL.

The robustness of DFree against ionosphere-related errors depends on the quality of the ionosphere monitor. This paper compared DFree and IFree under anomalous ionosphere conditions assuming a "perfect" ionosphere monitor for DFree. Although the assumption of a "perfect" ionosphere monitor unrealistically favors DFree, DFree achieved higher availability than IFree under anomalous conditions by only small amounts. This result suggests that, with a practical but imperfect ionosphere monitor, DFree might be inferior to IFree for most anomalous ionosphere conditions.

Based on these results, this paper introduces the hybrid dual-frequency LAAS concept in which the ionosphere monitor triggers switching from DFree to IFree in both ground and airborne systems under sufficiently anomalous ionosphere conditions. In theory, this method optimizes overall availability by using DFree most of the time and switching to IFree only when DFree integrity requires a larger error bound than IFree does. Future work on this concept will focus on investigating the performance of DFree with a practical ionosphere monitor that can realistically be implemented. By doing this, it will be possible to identify the optimal choice between DFree and IFree for any realizable state of the ionosphere monitor.

ACKNOWLEDGEMENTS

The authors would like to thank several people who helped with this paper and the work that it covers, including Ming Luo, Seebany Datta-Barua, Jiyun Lee, and Peggy Brister. The authors would also like to thank the Federal Aviation Administration LAAS Program Office for supporting this research. The opinions discussed in this paper are those of the authors and do not necessarily represent those of FAA or other affiliated agencies.

REFERENCES

[1] M. Luo, S. Pullen, et al., "Ionosphere Threat to LAAS: Updated Model, User Impact, and Mitigations," *Proceedings of ION GNSS 2004*, Long Beach, CA., Sept. 21-24, 2004.

[2] T. Walter, S. Datta-Barua, et al., "The Effects of Large Ionospheric Gradients on Single Frequency Airborne Smoothing Filter for WAAS and LAAS," *Proceedings of ION National Technical Meeting*, San Diego, CA., January, 2004

[3] P. Hwang, G. McGraw, J. Bader, "Enhanced Differential GPS Carrier-Smoothed Code Processing Using Dual-Frequency Measurements," *Navigation*. Vol. 46, No. 2, Summer 1999, pp. 127-137.

[4] J. Stevens, C. Varner, *et al*., "LDGPS Performance Assessment Using the JPALS Availability Model," *Proceedings of ION GNSS 2004*, Long Beach, CA., Sept. 21-24, 2004.

[5] G. McGraw, P. Young, "Dual Frequency Smoothing DGPS Performance Evaluation Studies," *Proceedings of ION National Technical Meeting*, San Diego, CA., Jan. 24-26, 2005.

[6] G. McGraw, T Murphy, *et al*., "Development of the LAAS Accuracy Models," *Proceeding of ION GPS 2000*, Salt Lake City, UT., Sept. 19-22, 2000.

[7] *Minimum Aviation System Performance Standards for Local Area Augmentation System (LAAS)*. Washington, D.C., RTCA SC-159, WG-4A, DO-245A, Dec. 9, 2004.

[8] C. Shively, T. Hsiao, "Availability Enhancements for CAT IIIB LAAS," *Navigation*. Vol. 51, No. 1, Spring, 2004, pp. 45-57.

[9] J. Rife, S. Pullen, "The Impact of Measurement Biases on Availability for CAT III LAAS," *Proceedings of ION Annual Meeting*, Cambridge, MA., June, 2005.

[10] *Minimum Operational Performance Standards for Global Positioning System/Wide Area Augmentation System Airborne Equipment*. Washington, D.C., RTCA SC-159, WG-2, DO-229C, Nov. 28, 2001.

[11] T. Murphy, M. Harris, "More Results from the Investigation of Airborne Multipath Errors," *Proceedings of ION GNSS 2005*, Long Beach, CA., Sept. 13-16, 2005.

[12] S. Datta-Barua, T. Walter, et al., "Using WAAS Ionospheric Data to Estimate LAAS Short Baseline Gradients," *Proceedings of ION National Technical Meeting*, San Diego, CA., January, 2002.

[13] A. Ene, D. Qiu, *et al*., "A Comprehensive Ionosphere Storm Data Analysis Method to Support LAAS Threat Model Development," *Proceedings of ION National Technical Meeting*, San Diego, CA., Jan. 24-26, 2005.

[14] T. Dehel, F. Lorge, *et al*., "Satellite Navigation vs. the Ionosphere: Where Are We, and Where Are We Going?," *Proceedings of ION GNSS 2004*, Long Beach, CA., Sept. 21-24, 2004.

[15] T. Murphy, "Development of Signal in Space CAT II / III Landing Operations," *Proceedings of ION GPS 2002*, Portland, OR., Sept. 24-27, 2002.